

# THE VERGE OF CURLING: NUMERICAL AND EXPERIMENTAL COMPARISON OF SPINNAKER AERODYNAMICS

**B. Augier**, IFREMER, Wave&Wind tank, Brest, France, benoit.augier@ifremer.fr

**B. Paillard**, Alternative Current Energy, Bordeaux, France, benoit.paillard@alternativecurrentenergy.com

**M. Sacher**, ENSTA Bretagne, CNRS UMR 6027, IRDL, Brest, France, matthieu.sacher@ensta-bretagne.fr

**J.B. Leroux**, ENSTA Bretagne, CNRS UMR 6027, IRDL, Brest, France, jean-baptiste.leroux@ensta-bretagne.fr

**N. Aubin**, Doyle Sails, Auckland, NZ, nicolas.research.aubin@gmail.com

The “verge of curling” recommendation is one of the common advice that sailors follow for efficient sailing downwind with a spinnaker. Wind tunnel experiments on spinnaker models conducted by [Aubin et al., 2017] in the Twisted Flow Wind Tunnel of the Yacht Research Unit of the University of Auckland have shown that curling can be related to better performance at Apparent Wind Angle  $\geq 100^\circ$ . In the present article, we will focus on the aerodynamic performance jump observed at Apparent Wind Angle  $AWA = 100^\circ$ , where the drive force increases up to 15% when the sail starts to flap. Thanks to four triggered HD cameras and coded targets stuck on the sail, three flying shapes of the spinnaker are reconstructed by photogrammetry for different sheet lengths from over trimmed to flapping occurrence. The pimpleFOAM solver from OpenFOAM is used to simulate the aerodynamic for the three rigid extracted flying shapes. Results highlight the ability of the model to simulate the experimental jump observed closed to curling and the significant confinement effect of the roof of the wind tunnel.

## NOMENCLATURE

$C_{Fy}$	Side Force coefficient
$C_{Fx}$	Drive Force coefficient
$L_{sheet}$	Sheet length
$U_x$	flow velocity in the x direction ( $m.s^{-1}$ )
AWA	Apparent Wind Angle ( $^\circ$ )

## 1 INTRODUCTION

The “verge of curling” recommendation is one of the most common pieces of advice that sailors follow for efficient sailing downwind with a spinnaker. Full-scale tests, thanks to the VOILENav project and the Sailing Fluids program, have recently investigated this complex unsteady Fluid-Structure Interaction phenomenon based on pressures and flying shape measurement [14, 7, 6]. These results show that the curling of the leading edge of the spinnaker is associated with a pressure field evolution, which propagation generates high suction peaks on the luff area. Arredondo and Viola [1] newly studied similar behavior with the Leading Edge Vortex (LEV) flow pattern. In a recent study Aubin et al. [2], wind tunnel experiments on a spinnaker are conducted in Twisted Flow Wind Tunnel (TWFT) [11] of the Yacht Research Unit of the University of Auckland measuring simultaneously aerodynamic forces, sheet length, sheet load, and flying shape recorded by four triggered HD cameras (Fig. 1). [2] has shown that curling can be related to better performance at Apparent Wind Angle  $\geq 100^\circ$ .

In the present article, we will focus on the aerodynamic performance jump observed at  $AWA = 100^\circ$  (Fig. 2), where the drive force increases up to 15% just before the sail starts to flap. The question asked here is: **can we simulate this observed increase?**

To better assess the aerodynamic performance of downwind sail, Viola [19, 20] has numerically provided

insights into the flow behavior, in particular in the luff area. Numerical simulations have also been performed on a fixed sail shape validated with wind tunnel experiments on flexible [21, 22, 23] and semi-rigid sails [4, 5]. Nonetheless, the realistic fluid-structure interaction simulations of downwind sails represent a significant step forward.

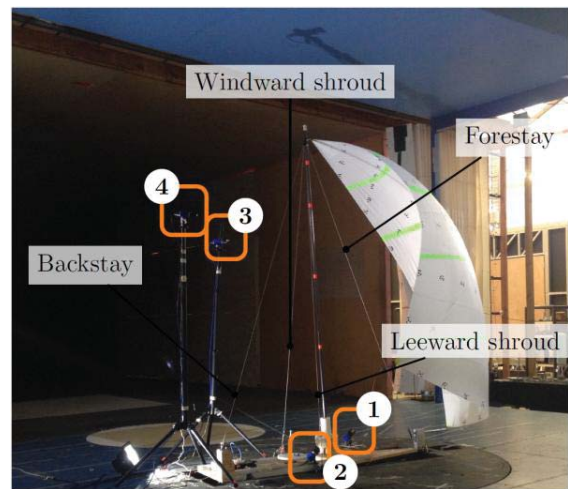


Figure 1: Experimental set up in the TFWT, Auckland, to measure the aerodynamic loads and spinnaker flying shape. The orange squares highlight the 4 photogrammetry cameras.

The step is in considering the significant influence of the added mass and simulating the curling of the luff, which is challenging mostly due to substantial displacements of the sail, requiring specific and complex mesh deformation methods. As a first approach, a finite element method has been coupled to a flow solver [16, 17, 18] to predict the sail flying shape in static simulations. Lombardi et al. [12] and Durand et al. [8, 9, 10] successfully achieved unsteady fluid-structure interaction simulations. Still, so

far, such simulations have not been compared to full-scale or wind tunnel experimental unsteady data, such as the dynamic curling behaviour at a fixed trim.

The problem is simplified here by considering 3 rigid flying shapes of the spinnaker reconstructed by photogrammetry [6] for different sheet lengths from over-trimmed to flapping occurrence.

Unsteady RANSE simulations using the pimpleFOAM solver from OpenFOAM are achieved on these rigid geometries and compared with experimental results. Authors believe that URANSE can simulate the aerodynamics of spinnaker with an appropriate mesh correctly, contrarily to previous studies [13, 15] where these models underestimate the aerodynamic loads.

The first part described the wind tunnel experimental set up and the flying shape recovery. The URANSE numerical model is then presented together with mesh characteristics. Simulation results are eventually compared to the experiment looking at the sensitivity of confinement and apparent wind angle.

## 2 EXPERIMENTAL APPARATUS

The presented experimental apparatus is part of a more extensive set up described in detail in [2, 3]. The purpose of the set up is here to link the aerodynamic performances to the so-called “flying shape” for different sail trims.

### 2.1 DRIVING FORCE MEASUREMENT

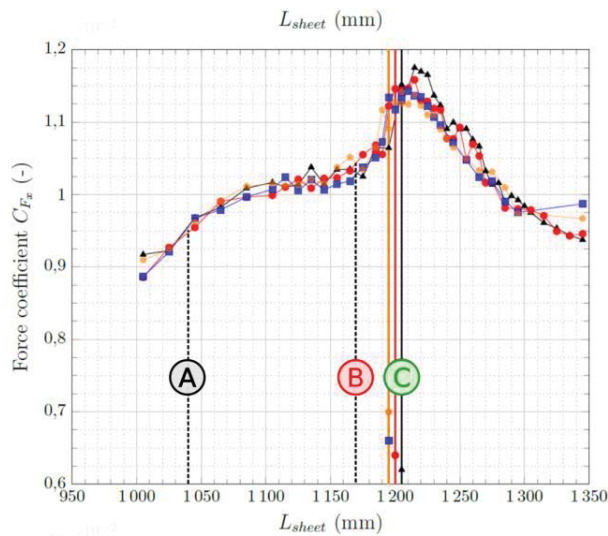


Figure 2: Evolution of driving force coefficient with the sheet length measured in the TFWT at AWA = 100° and  $U = 3.24\text{ms}^{-1}$  [Aubin et al., 2017]. A, B, and C refer to the 3 studied cases. Solid vertical lines represent flapping occurrence.

A 6DoF attached to the floor and connected to the model measures the forces. The AWA is modified thanks to a turning table, levelled with the floor. The balance turns with the table, linking then the measurement axis with the model axis.

The driving force coefficient is defined as the normalized force in the forward longitudinal axis of the boat when the side force coefficient is in the lateral axis (portside).

At fixed AWA, the sheet length has a significant effect on the driving force (Fig. 2). When easing the sheet, the driving force increases until reaching a maximum at the verge of curling. Colored vertical lines in Figure 2 indicate curling appearance. It is important to notice that the driving force jump is observed for all studied wind speed and spinnakers.

### 2.2 FLYING SHAPE MEASUREMENT

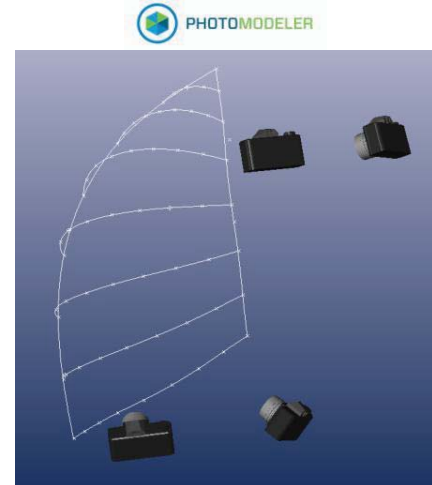
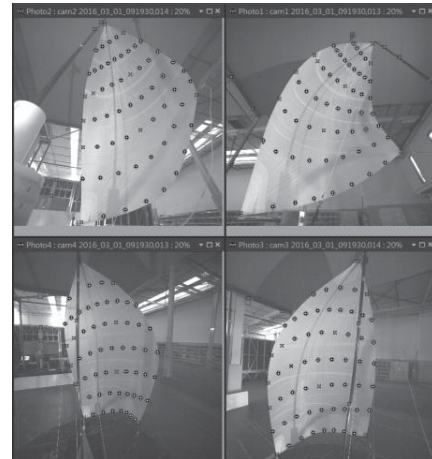


Figure 3: Flying shape reconstruction by photogrammetry with Photomodeler software.

#### 2.2.1 Photogrammetry set up

The flying shape of the spinnaker is significantly impacted by the sail trimming, even with a constant AWA. The geometry of the sail is extracted thanks to the photogrammetry technique using the Photomodeler Software. Four HD cameras - with locations as shown in Fig. 1 - record 2046x2046 black and white photographs at 20fps. Cameras are synchronized with the load balance. 51 coded targets are stuck on the sail (Fig. 3, top view), dividing the sail into 7 lines. Markers are also stuck in the wind tunnel walls and ceiling as a coordinate system and scale reference. Markers 3D positions are extracted using

Photomodeler software (Fig. 3) and exported on Rhinoceros 3D to built a surface.

The extracted geometries are, by nature, static representations of a dynamic phenomenon. The group of pictures defined for the post-processing is chosen arbitrarily to best represent the flying shape of the sail at a fixed sheet length. This hypothesis is good for over trimmed sails but starts to be questionable close to curling where the sail moves.

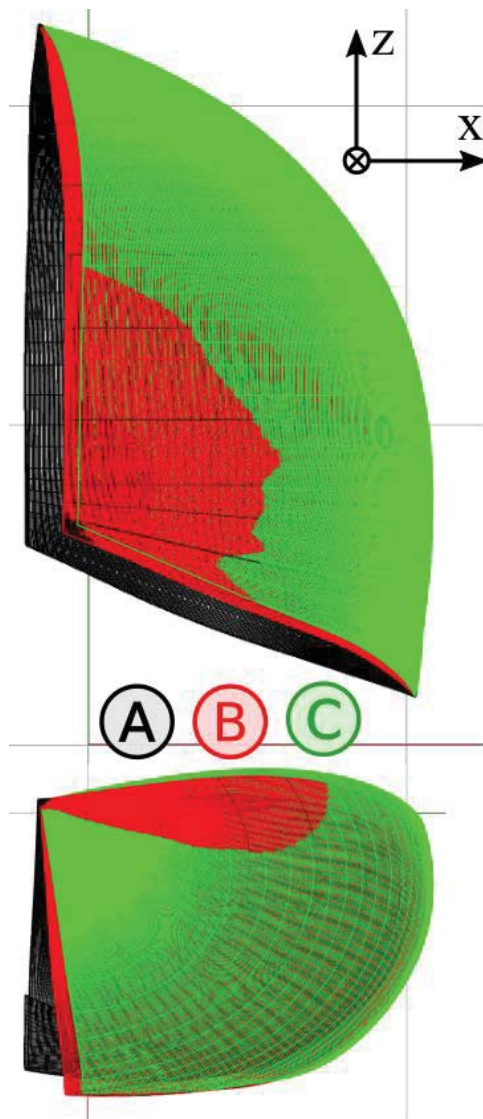


Figure 4: Comparison of the 3 extracted flying shapes

### 2.2.2 Definition of the studied cases

Three different cases are defined for the study. The cases are chosen to represent the full range of aerodynamic performance of the spinnaker (Fig. 2), from over trimmed to the verge of curling:

- A.  $L_{\text{sheet}} = 1045\text{mm} \rightarrow$  Spinnaker over trimmed
- B.  $L_{\text{sheet}} = 1165\text{mm} \rightarrow$  End of low  $C_{Fx}$  variation
- C.  $L_{\text{sheet}} = 1195\text{mm} \rightarrow$  On the verge of curling

As illustrated in Figure 4, the sheeting point moves forward and upward when easing the sail, when the luff is sliding windward. The 3 geometries are exported in .stl files as thick surfaces (1mm thickness) for the simulations. Geometries are available online [27].

## 3 NUMERICAL MODELS

### 3.1 OpenFOAM

The parallel incompressible viscous flow solver OpenFOAM, is used to solve the Unsteady Reynolds-Average Navier-Stokes Equations (URANS). The pressure-velocity coupling is achieved with a SIMPLE algorithm, and the standard two equations shear stress transport (SST) model [25] is presently used for turbulence modelling.

A parallelepiped computational domain enclosing the spinnaker is considered with extensions [-20 m, 80 m] x [-10 m, 10 m] x [0 m, 3.5 m] in X, Y and Z directions respectively. This domain is illustrated in Figure 5, where boundary conditions that are applied to the different domain faces are also provided. In particular, a uniform velocity of 3.25 m/s aligned with the X-axis is prescribed at the inlet plane. At the top and bottom planes, wall-function boundary conditions are used to model the roof and floor of the wind tunnel. Spinnaker surfaces are no-slip boundary conditions, and at the remaining outlet planes, the pressure is prescribed to zero.

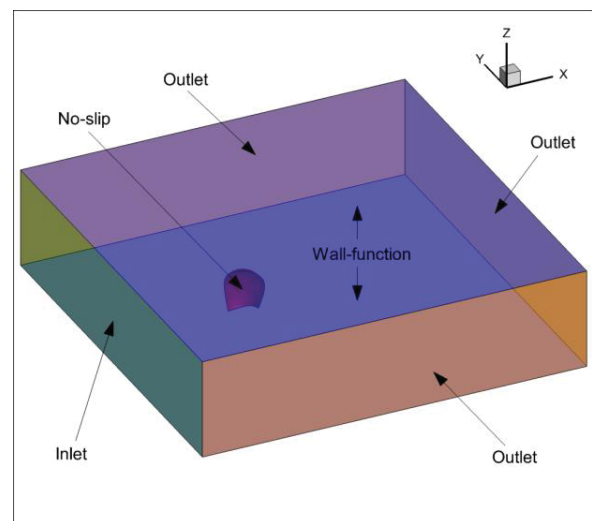


Figure 5: Computational domain with boundary conditions (domain extensions are not to real scale)

The fluid domain is meshed using the unstructured automatic mesh generator Cf-Mesh. The meshed domain is built with hexahedral cells (Fig. 6 - 7), except in regions close to spinnaker edges where prismatic cells are generated to allow an accurate boundary layer modelling. First cell thicknesses of domain regions with wall-type boundary conditions are set according to  $y^+$  criteria. Individually, it has been considered a  $y^+$  value of 80 for wall function boundary conditions. For no-slip boundary conditions on spinnaker surfaces, a value of  $y^+ < 5$  is ensured on the whole surface, leading to first layer

thicknesses of about 0.7 mm. This  $y^+$  value is determined after a convergence study and insures to keep the mesh size and quality at the optimal value. A mesh refinement box with a target cell size of 50 mm and extensions [-1.2 m, 6 m] x [-1.2 m, 2.5 m] x [0 m, 3 m] in X, Y and Z directions respectively, is also set in order to capture better spinnaker wake flows. The total number of cells is about 12 million, and the computing time on a high-performance cluster using 64 CPUs is about 1 CPUh per second.

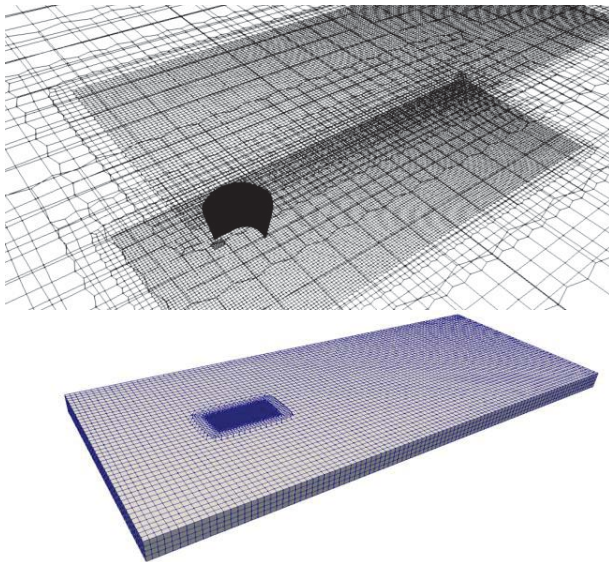


Figure 6: Unstructured mesh of the domain and refinement box around the spinnaker.

#### 4 RESULTS

Previous numerical studies made on the TFWT [22, Nava et al. 2017] have chosen a detailed modelling of the tunnel inlet condition. In this study, we only focus on two geometrical parameters: the AWA and the effect of the roof. These parameters have from the authors' experiences in Auckland's wind tunnel, the most significant effect on the results. Sensitivity with AWA without modelling the Z confinement, i.e. the roof of the tunnel is first investigated. The effect of Z confinement is then studied.

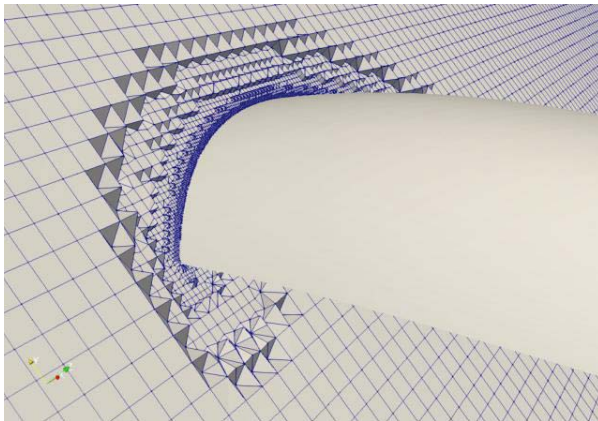


Figure 7: Mesh refinement around the sail highlighting the boundary layers

#### 4.1 Sensitivity to AWA

In the TFWT, a turning table helps to set the AWA [11]. This angle setting is very sensitive to the users and could significantly differ from a campaign to another by  $\pm 5^\circ$ . This precision is considered in the simulations where 3 AWA are computed, i.e.  $95^\circ$ ,  $100^\circ$ , and  $105^\circ$ . The sensitivity of aerodynamic coefficients to AWA is then studied.

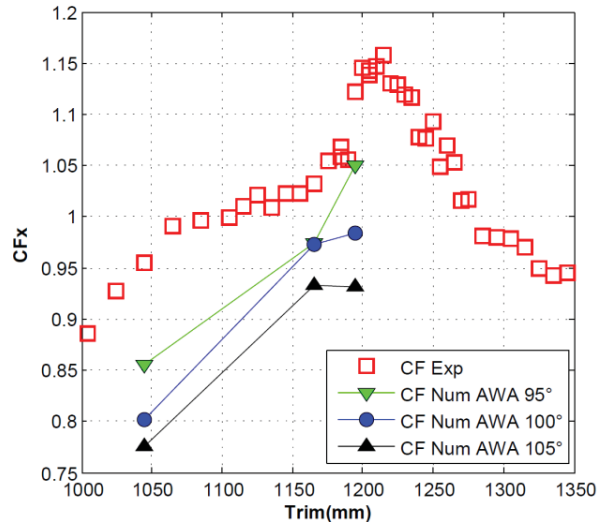


Figure 8:  $CF_x$  as a function of the trim for different AWA using an outlet condition on the top domain plane

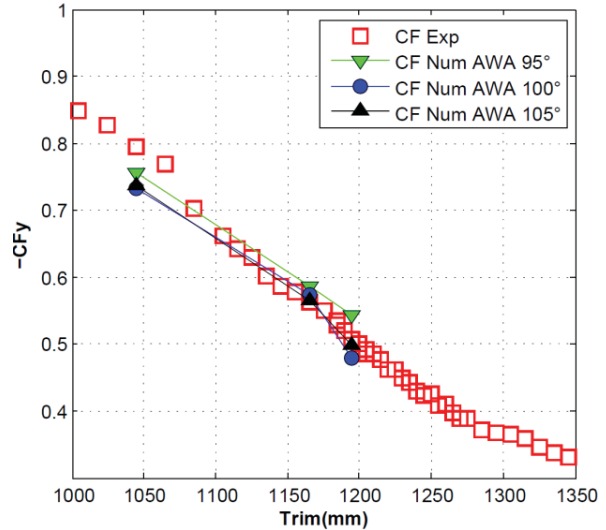


Figure 9:  $-CF_y$  as a function of the trim for different AWA using an outlet condition on the top domain plane

The evolution of the aerodynamic coefficients with trim is represented in Figures 8 and 9 for different computed AWA. The comparison highlights the sensitivity of the driving force and side force to the considered apparent wind. The aerodynamics forces increase when the AWA decreases as a direct consequence of the decrease of the angle of attack at the sail's leading edge. For  $AWA = 95^\circ$ , a clear jump in the driving force is observed between case B and C when a plateau is computed for  $100^\circ$  and  $105^\circ$ .

4.2 Sensibility to Z confinement

In the TFWT test section, the only remaining walls are the floor and the roof. The foot of the sail is at 0.15m of the deck, and the floor is simulated. The influence of the roof on the aerodynamic performance is studied to quantify the confinement effects of the tunnel, Sail's head is at 2.37m when the testing section height is  $Z = 3.5\text{m}$ . The case  $\text{AWA} = 95^\circ$  is the only considered case in the following discussion. As illustrated in Figures 10 and 11, considering the roof affects the results, increasing the aerodynamic coefficients. Several quantities are presented in the following to understand the effect of trim on the aerodynamics.

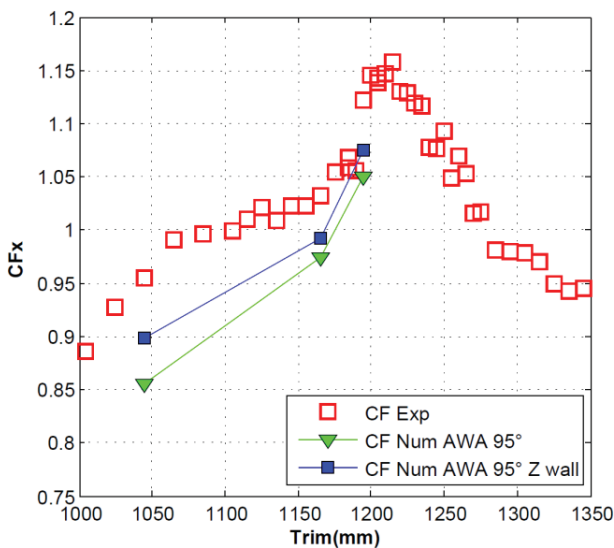


Figure 10:  $CF_x$  as a function of the trim using a wall-function condition on the top domain plane

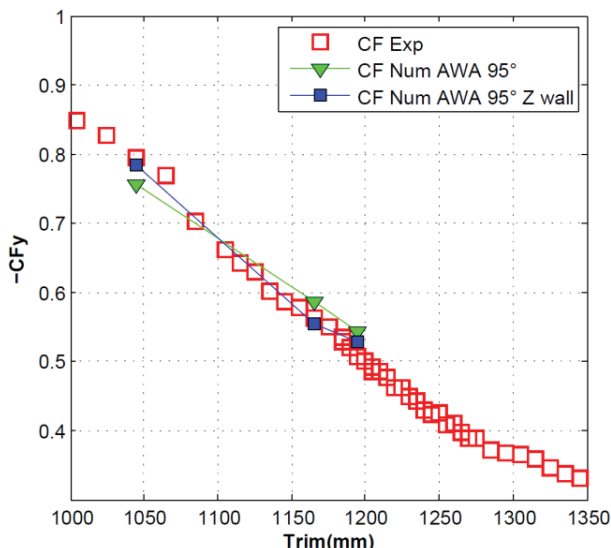


Figure 11:  $-CF_y$  as a function of the trim using a wall-function condition on the top domain plane

4.2.1 Pressure distributions

Pressure distributions on the spinnaker are represented with streamlines for the 3 different flying shapes in Figures 15 and 17. From these figures, an apparent augmentation of the suction area is observed when easing the sail. The suction area is focused near the top leading edge. It is interesting to notice that, from cases B to C, suction peak moves from a stripe linked to the leading edge to a larger area not connected to the sail edge. This translation of the suction peaks leads to an important pressure gradient, which overlaps to the sail area where curling appears.

The confinement has no apparent impact on the general map of the pressure distribution. However, it affects the maximum low-pressure area where the suction peak is extended, and the magnitude increased. The effect is then limited to the top of the sail, as expected, but with a significant impact on the global performance regarding the suction peak position.

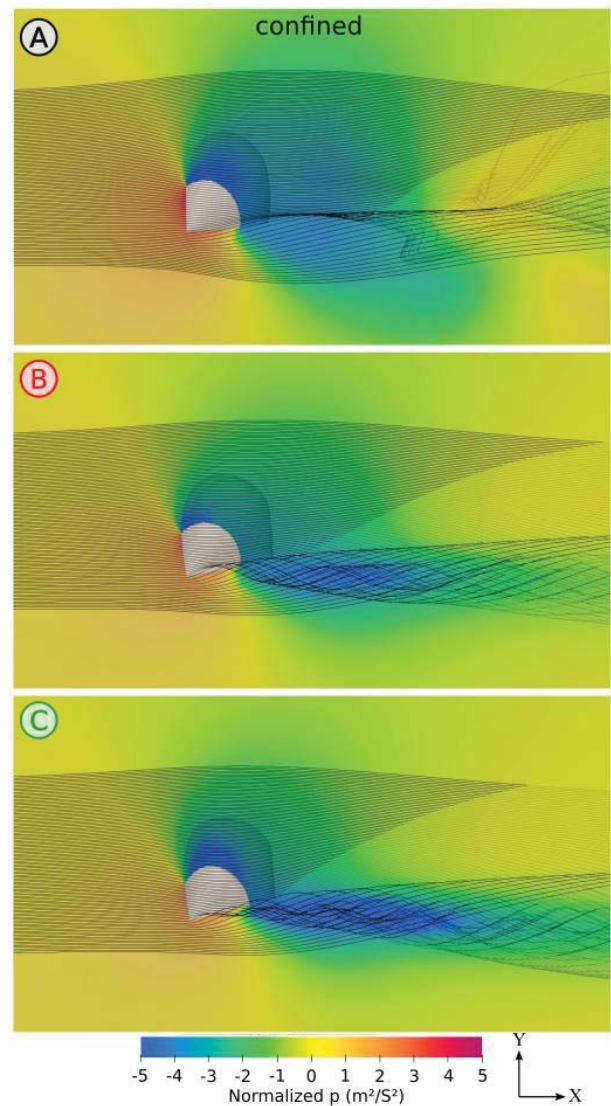


Figure 12: Normalized pressure in the plan  $Z=1.85$  for the different trimming using a wall-function condition on the top domain plane (OpenFOAM URANS –  $k-\omega$  sst)

#### 4.2.2 Velocity

Velocity  $U_x$  is plotted for the different flying shapes in the YX plan ( $Z=1.85\text{m}$ ) in Figures 12 and 13 and the ZX plan in Figures 14 and 16, respectively, without and with confinement. First, the ZX representation illustrates the importance of the confinement effect due to the modelling of a wall at the roof. The over speeds observed up to the roof in the confinement case are limited to the really top of the sail in the outlet case. Second, the trim has an important effect on the downstream domain. When easing the sail, the low-speed area downstream of the spinnaker decreases and condenses to the bottom part. Eventually, streamlines of the ease case C are more aligned with the upstream flow, when case A seems to be subject to more significant and stronger turbulent structures.

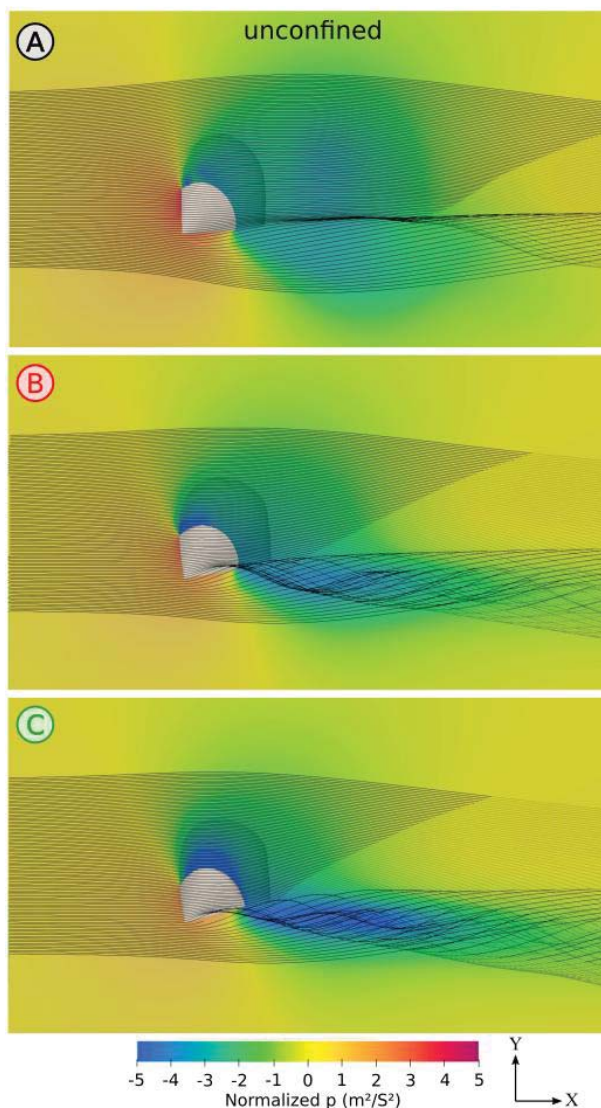


Figure 13: Normalized pressure in the plan  $Z=1.85$  for the different trimming using a pressure outlet condition on the top domain plane (OpenFOAM URANS –  $k-\omega$  sst)

In the YX plan, the evolution of the suction peak is clearly visible in the domain with an important low-pressure area near the leading edge, getting more prominent when the sail is eased.

## 5 CONCLUSIONS

In this article, a numerical model has been set up to compute URANSE simulation of spinnakers for different trimming. These simulations are compared to experimental data measured in wind tunnel where a jump was observed on the verge of curling. The results of numerical and experimental comparisons can be presented in four points:

- A URANSE approach based on pimpleFOAM solver from OpenFOAM is able to simulate the aerodynamic performance of a spinnaker correctly and to compute the observed drive force jump close to curling
- The AWA has a strong influence on the simulation results, especially on drive force jump modelling
- The confinement effect has a limited effect on the global pressure distribution but influences greatly the spinnaker suction peak located at the top of the sail
- On the verge of curling, the suction peak moves from the leading edge to the centre of the sail, creating a relatively high pressure that is overlapping the curling part.

Further work will concern a focused study on the jump appearance at trim C. Specifically, it is intended to investigate in more detail the jump appearance as a function of the AWA. A grid sensitivity analysis is planned as well as taking into account the walls of the wind tunnel at the computation domain velocity inlet plane [Viola et al., 2013, Nava et al., 2017]. URANSE-LES computations may also be conducted in future works.

## ACKNOWLEDGEMENTS

The experimental work presented was supported by Brest Métropole Océane, the French Naval academy, and has received fundings from the European Union's Seventh Program SAILING FLUIDS, noPIRSES-GA-2012-318924.

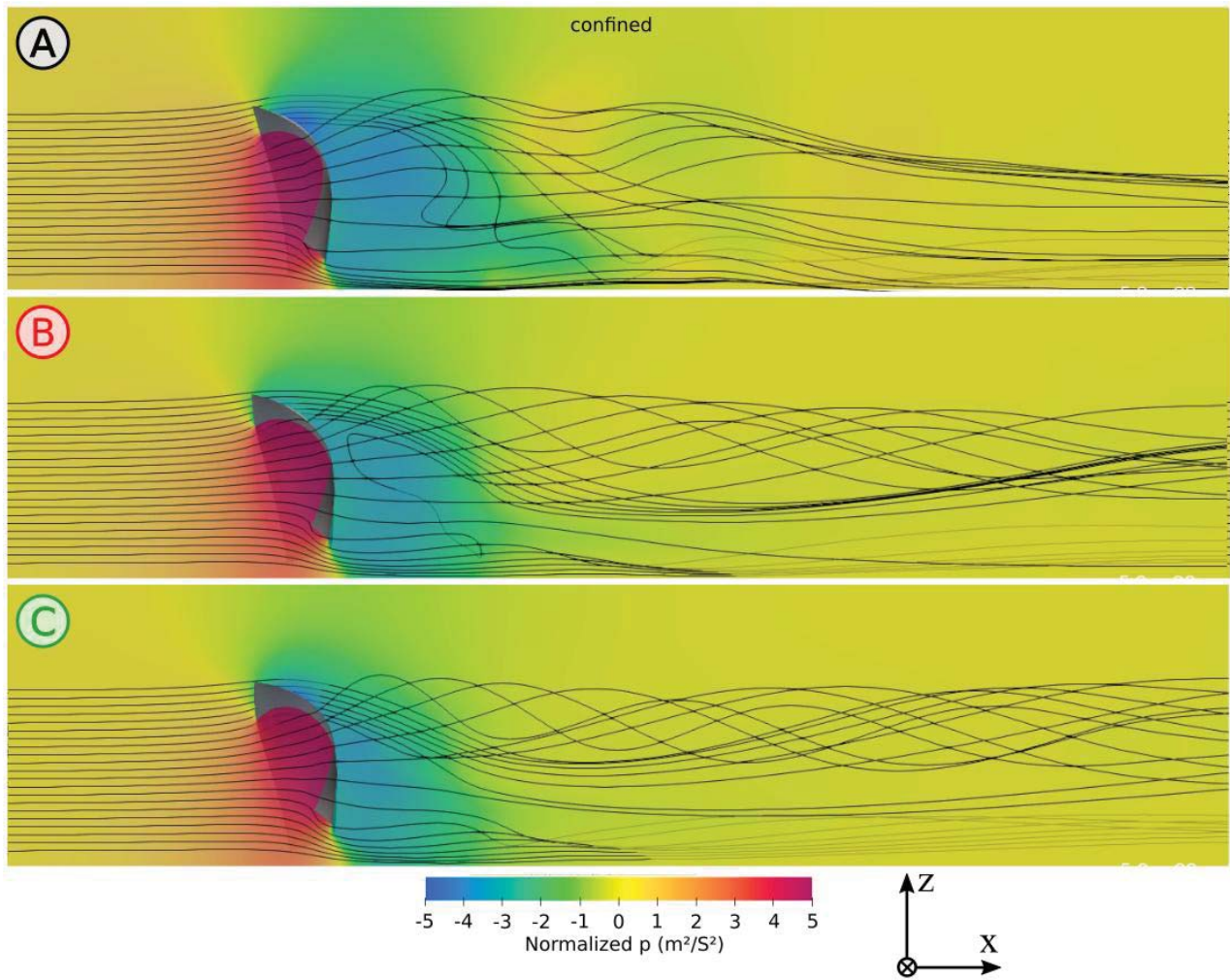


Figure 14: Ux for different spinnaker trimming using a wall-function condition on the top domain plane (OpenFOAM URANS – k- $\omega$  sst)

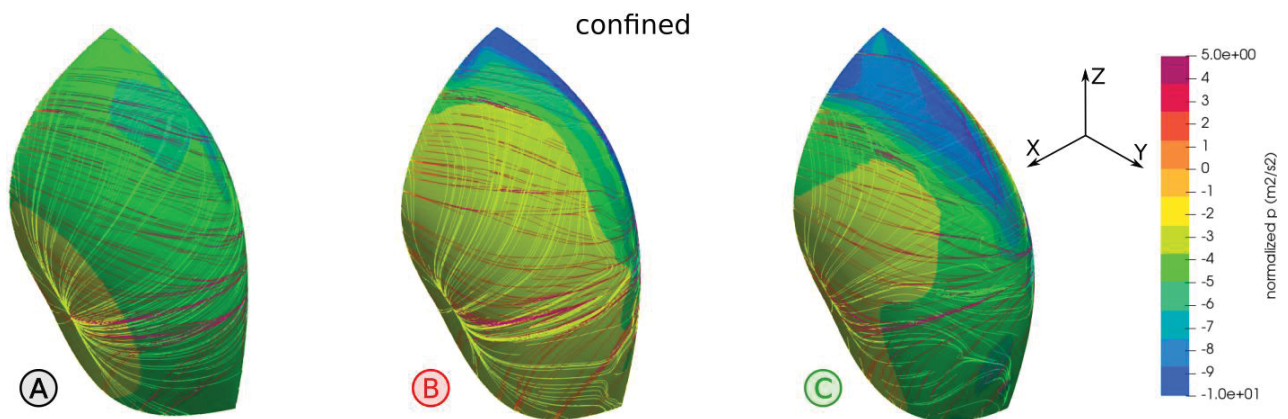


Figure 15: Pressure differences on the spinnaker for the different trimming using a wall-function condition on the top domain plane (OpenFOAM URANS – k- $\omega$  sst)

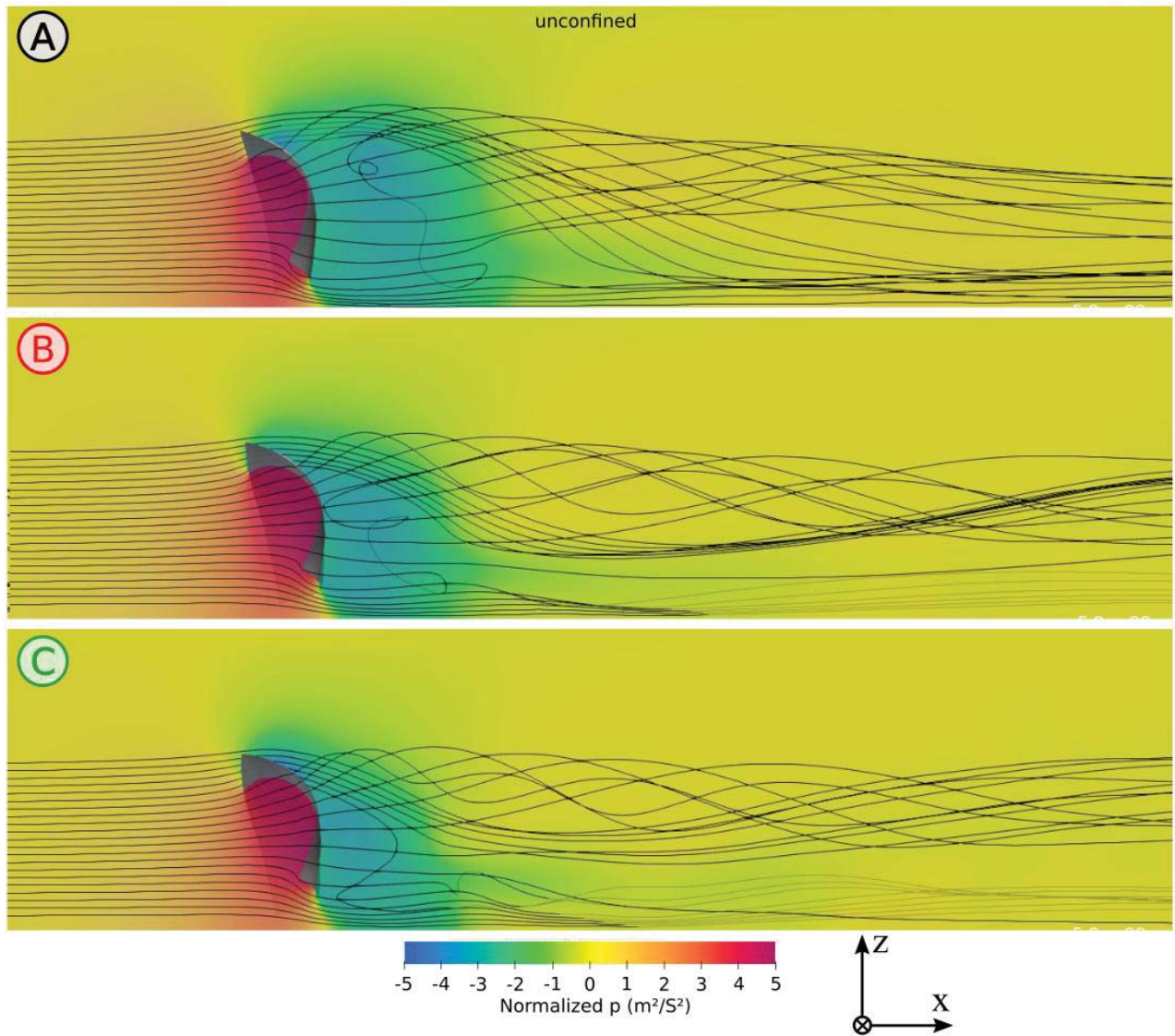


Figure 16:  $U_x$  for different spinnaker trimming using a pressure outlet condition on the top domain plane (OpenFOAM URANS –  $k-\omega$  sst)

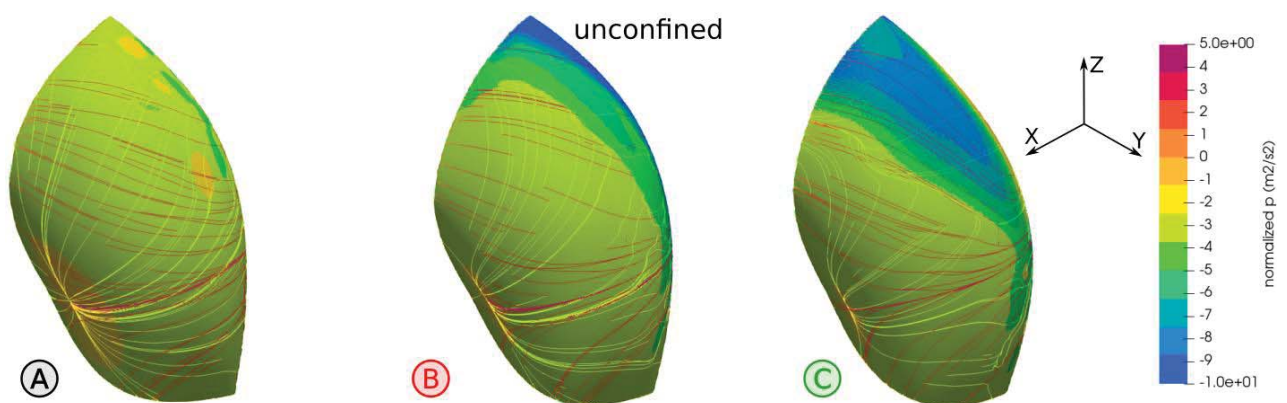


Figure 17: Pressure differences on the spinnaker for the different trimmings using a pressure outlet condition on the top domain plane (OpenFOAM URANS –  $k-\omega$  sst)

## REFERENCES

1. A. Arredondo and I. M. Viola. On the leading edge vortex of thin wings. In 69th Annual meeting of the APS Division of Fluid Dynamics Meeting Abstracts, volume 61, Portland, Oregon, USA, 2016.
2. N. Aubin, B. Augier, J. Deparday, and M. Sacher (2017). To curl or not to curl: wind tunnel investigation of spinnaker performance. In *Conference on Innovation in High Performance Sailing Yachts INNOVSAIL 2017*, Lorient, France.
3. N. Aubin, (2017) Fluid-structure interaction on yacht sails: from full-scale approach to wind tunnel unsteady study. *PhD Thesis*
4. P. Bot, I. M. Viola, R. G. J. Flay, and J.-s. Brett. Wind-Tunnel pressure measurements on model-scale semi rigid downwind sails. In The Third International Conference on Innovation in High Performance Sailing Yachts (Innovsail), pages 119–127, Lorient, France, 2013.
5. P. Bot, I. M. Viola, R. G. J. Flay, and J.-S. Brett. Windtunnel pressure measurements on model-scale rigid downwind sails. *Ocean Engineering*, 90:84–92, 2014.
6. J. Deparday. Experimental studies of Fluid-Structure Interaction on Downwind Sails. PhD thesis, Université de Bretagne Occidentale, Brest, 2016.
7. J. Deparday, B. Augier, P. Bot (2018). Experimental analysis of a strong fluid–structure interaction on a soft membrane—Application to the flapping of a yacht downwind sail. *Journal Of Fluids And Structures*, 81, 547-564
8. M. Durand, F. Hauville, P. Bot, B. Augier, Y. Roux, A. Leroyer, and M. Visonneau. Unsteady numerical simulations of downwind sails. In International Conference on Innovation in High Performance Sailing Yachts, Lorient, France, 2010.
9. M. Durand. Interaction fluide-structure souple et légère, applications aux voiliers. PhD thesis, Ecole Centrale de Nantes, 2012.
10. M. Durand, A. Leroyer, C. Lothodé, F. Hauville, M. Visonneau, R. Floch, and L. Guillaume. FSI investigation on stability of downwind sails with an automatic dynamic trimming. *Ocean Engineering*, 90:129–139, 2014.
11. R. G. J. Flay. A twisted flow wind tunnel for testing yacht sails. *Journal of Wind Engineering and Industrial Aerodynamics*, 63(1-3):171–182, 1996.
12. M. Lombardi, M. Cremonesi, A. Giampieri, N. Parolini, and A. Quarteroni. A strongly coupled fluid-structure interaction model for wind-sail simulation. In 4th High Performance Yacht Design, pages 212–221, Auckland, New Zealand, 2012.
13. W.C. Lasher, J.R. Sonnenmeier: An Analysis of Practical RANS Simulations for Spinnaker Aerodynamics, *Journal of Wind Engineering and Industrial Aerodynamics*, v. 96, pp. 143–165. (2008).
14. D. Motta, R. G. J. Flay, P. J. Richards, D. J. Le Pelley, J. Deparday, and P. Bot. Experimental investigation of asymmetric spinnaker aerodynamics using pressure and sail shape measurements. *Ocean Engineering*, 90:104–118, 2014.
15. S. Nava, J. Cater, and S. Norris (2017). Large eddy simulation of downwind sailing. In *Conference on Innovation in High Performance Sailing Yachts INNOVSAIL 2017*, Lorient, France.
16. H. Renzsch and K. Graf. Fluid-structure interaction simulation of spinnakers - getting close to reality. In The Second International Conference on Innovation in High Performance Sailing Yachts, Lorient, France, 2010. Royal Institution of Naval Architects.
17. H. Renzsch and K. Graf. An experimental validation case for fluid-structure-interaction simulations of downwind sails. In The 21st Chesapeake Sailing Yacht Symposium, Annapolis, Maryland, USA, 2013.
18. D. Trimarchi, M. Vidrascu, D. Taunton, S. Turnock, and D. Chapelle. Wrinkle development analysis in thin sail-like structures using MITC shell finite elements. *Finite Elements in Analysis and Design*, 64:48–64, 2013.
19. M. Viola. Downwind sail aerodynamics: A CFD investigation with high grid resolution. *Ocean Engineering*, 36(12):974–984, 2009.
20. M. Viola, S. Bartesaghi, T. Van-Renterghem, and R. Ponzini. Detached Eddy Simulation of a sailing yacht. *Ocean Engineering*, 90:93–103, 2014.
21. M. Viola and R. G. J. Flay. Force and Pressure Investigation of Modern Asymmetric Spinnakers. *International Journal of Small Craft Technology*, 151, 2009.
22. M. Viola and R. G. J. Flay. Sail pressures from fullscale, wind-tunnel and numerical investigations. *Ocean Engineering*, 38(16):1733–1743, 2011.
23. M. Viola and R. G. J. Flay. Pressure distributions on modern asymmetric spinnakers. *International Journal of Small Craft Technology*, 152(1):41–48, 2015.
24. I.M. Viola, P. Bot, M. Riotte. Upwind sail aerodynamics: A RANS numerical investigation validated

with wind tunnel pressure measurements, International Journal of Heat and Fluid Flow, (39) 90-101, 2013

25. F.R. Menter, M. Kuntz, R. Langtry, 2003. Turbulence heat and mass transfer. Ten years Ind. Exp. SST Turbul. Model 4, 625–632.

27. STEP Geometries are available [here](#)

## **AUTHORS BIOGRAPHY**

**B. Augier** holds the current position of Researcher at IFREMER, France. He is the Brest Wave&Wind Tank Manager and his leading different projects on Floating Offshore Wind Turbine and Fluid Structure Interaction of composite hydrofoils. His previous experience includes sailing yacht onboard instrumentation, wind tunnel testing and hydrodynamic study of hydrofoils.

**B. Paillard** hold the current position of head of research at Alternative Current Energy. He studied mechanical engineering at ENSAM ParisTech before graduating in applied aerodynamics and modelization at Jussieu university Paris 6. He worked as a research assistant at UC Davis under the direction of Prof. Chattot on fluid structure interaction applied to wind turbine blades. This led him to carry out a PhD on variable pitch crossflow wind turbines at French Naval Academy Research Institute, which he defended in 2011. He has been working as a consultant for many academic and industrial projects involving crossflow turbines since then.

**M. Sacher** holds the current position of Assistant Professor at the graduate and postgraduate school of engineering, Ecole Nationale Supérieure de Techniques Avancées Bretagne (ENSTA Bretagne), Brest, Brittany, France.

**JB. Leroux** holds the current position of Associate Professor at the graduate and postgraduate school of engineering, Ecole Nationale Supérieure de Techniques Avancées Bretagne (ENSTA Bretagne), Brest, Brittany, France. He is co-responsible for the Naval and Offshore Architecture program and he is in charge of courses in Naval Hydrodynamics fields. His previous experience includes hydrodynamics and cavitation of lifting bodies.

**N. Aubin** holds the current position of R&D engineer at Stratis Doyle Sails in New Zealand. He is responsible for the development of new technology for membrane engineering and production. His previous experiences include a PhD from the University of Western Brittany, working on fluid structure interaction on yacht sails under unsteady conditions at the French Naval Academy Research Institute. He holds a Masters degree of engineering from the Ecole Centrale de Nantes and studied aerodynamic sailing fleet interferences at the Yacht Research Unit of the University of Auckland. His research interests include sail design and manufacturing (CFD, FSI, CNC machines).